



## Unlocking nature's arsenal: Exploring the molecular interactions of *Tinospora cordifolia* phytochemicals with anti-apoptotic receptor proteins

BY

Bandita Baruwa<sup>1</sup>, Akalesh Kumar Verma<sup>2\*</sup>, Namram Sushindrajit Singh<sup>3</sup>, Mamata Goswami<sup>4</sup>

<sup>1,2,3,4</sup>Department of Zoology, Cell & Biochemical Technology Laboratory, Cotton University, Panbazar-781001, Guwahati, Assam, India



### Article History

Received: 09/10/2023

Accepted: 06/11/2023

Published: 08/11/2023

Vol – 2 Issue – 11

PP: - 01-24

DOI:  
10.5281/zenodo.1018  
3684

### Abstract

Indigenous medicinal plants frequently undergo diverse experiments aimed at discovering new drugs. *Tinospora cordifolia* (TC), commonly known as Giloy, is a climbing plant primarily found in the Indian subcontinent and belongs to the Menispermaceae family. In the present study, a wide array of phytochemical compounds falling into categories such as alkaloids, steroids, sesquiterpenoids, diterpenoids, phenolics, aliphatic compounds, and polysaccharides, among others, as documented in various sources, were subjected to molecular docking with well-established receptors associated with cancer progression. The results revealed that certain phytochemical compounds, including syringin, neotigogenin, and cordifolin, displayed the high binding energy with different receptors such as solution structure of the anti-apoptotic protein Bcl-2 in complex with an acyl-sulfonamide-based ligand (2O22), structure of the BIR domain of IAP-like protein 2 (1XBO), structure of BIRC7-UbcH5b-Ub complex (4AUQ), and crystal structure of Human Hsp90 with RLI (4L8Z). Hence, it is reasonable to propose that these compounds may hold promise as potential anti-cancer agents, as they exhibit the potential to interfere with the activity of these receptors, potentially leading to their downregulation.

**Keywords:** Anticancer; bioactive compounds; Giloy; molecular docking; phytochemicals.

## 1. Introduction

Apoptosis, a vital biological process, is integral to normal development, maintaining tissue balance, and eliminating damaged or infected cells. Any disruption of this process can result in a wide range of human diseases (Agrawal, 2019). For instance, numerous types of cancer are characterized by an imbalance between pro-apoptotic and anti-apoptotic proteins, causing an accumulation of cells and an inadequate response to apoptotic triggers. Consequently, these cancer types often exhibit resistance to therapeutic approaches that rely on inducing apoptosis as a primary mechanism of action (Jan and Chaudhry, 2019).

### 1.1. Cancer and its allies:

#### 1.1.1. Bcl-2 family:

One important set of proteins involved in the regulation of apoptosis is the Bcl-2 family. Bcl-2 and other members of the family play an important role in embryogenesis, tissue remodeling, and the immune response through their actions as either inhibitors or promoters of apoptosis (Adams and Cory, 1998; Kelekar and Thompson, 1998; Chao and Korsmeyer, 1998). There are at least 16 Bcl-2 homologues found in humans (Reed, 1999). These include Bcl-2, Bcl-xL, Bcl-w,

and Mcl-1 which are inhibitors of cell death, and Bad, Bak, Bax, Bid, Bim, and Bcl-xS, which are cell-death promoters. Homeostasis is maintained in normal tissues through the antagonistic interaction of these anti- and pro-apoptotic proteins (Yang *et al.*, 1995). In addition to their normal function, aberrant expression of Bcl-2 proteins has been linked to many diseases such as auto-immunity and neurodegenerative disorders, and cancer (Thompson, 1995; Kusenda 1998; Strasser *et al.*, 1997). Indeed, Bcl-2 has been found to be overexpressed in many cancer cells, including most B cell-derived lymphomas, colorectal adenocarcinomas and undifferentiated nasopharyngeal cancers (Berghella *et al.*, 1998). Bcl-2 has been implicated also in the resistance of many cancers to treatment with radiation and chemotherapeutic agents (Reed, 1999; Kusenda, 1998). Therefore, Bcl-2 represents a target for the treatment of cancers, especially those in which Bcl-2 is over expressed and for which traditional therapy has failed (Berghella *et al.*, 1998; Nicholson *et al.*, 2000; Piche *et al.*, 1998; Wang *et al.*, 2000; Wang *et al.*, 2000).

#### 1.1.2. Ubiquitin ligases:

The progression of cancer is a complex, multistep journey during which normal cells gradually transition into a

neoplastic state. Along this transformation, they acquire various characteristics, including enhanced proliferation, improved survival capabilities, invasive potential, metastatic ability, and strategies to evade immune surveillance and destruction (Hanahan and Weinberg, 2011). Such a complex process requires the reprogramming of cellular signaling networks to meet the needs for malignant transformation. Ubiquitylation refers to the enzymatic post-translational modification in which the ubiquitin protein is covalently attached to cellular proteins (Hershko and Ciechanover, 1998). The core enzymes driving this process are the ubiquitin-activating enzyme (UAE or E1), the ubiquitin-conjugating enzyme (UBC or E2), and the ubiquitin ligase (E3). E3s recruit substrates and thus determine the overall specificity for ubiquitylation. They constitute a wide class of proteins, with the human genome encoding more than 600 putative E3s (Li et al., 2008). By controlling protein abundance and activity in a timely and specific manner, E3s serve as central regulatory nodes for many signaling pathways. It is therefore no surprise to observe that E3s and their substrates are frequently deregulated in human cancers (Qi and Ronai, 2015). Anomalies in the control of E3 ligases may arise at the genetic, epigenetic, or post-translational levels. Such modifications to E3 ligases can result in the conversion of proto-oncoproteins into oncoproteins or the inactivation of tumor suppressors.

#### 1.1.3. Inhibitor of Apoptosis-like protein:

The gene family encoding IAP (inhibitor of apoptosis) proteins, originally found in baculoviruses are present in organisms from viruses to yeast to humans (Hwain et al., 2005; Uren et al., 1998;). Their characteristic protein motif is the BIR (baculovirus IAP repeat), an approx. 80-amino-acid zinc-stabilized domain. Up to three tandem copies of the BIR domain can occur within the known IAP family proteins from viruses and animal species (reviewed in Deveraux and Reed, 1999; Salvesen and Duckett, 2002). There are currently eight human IAP proteins annotated in the Human Genome Nomenclature database: NAIP (neuronal apoptosis inhibitory protein), c-IAP1 (cellular IAP1), c-IAP2, XIAP (X-linked IAP), ML-IAP (melanoma IAP), ILP2 (IAP-like protein 2), survivin and BRUCE (BIR repeat-containing ubiquitin-conjugating enzyme) (reviewed in Deveraux and Reed, 1999). Several IAPs, including XIAP (Deveraux et al., 1997) and multiple references in Salvesen and Duckett, 2002), c-IAP1 (Roy et al., 1997) c-IAP2 (Roy et al., 1997), NAIP (Maier et al., 2002), ML-IAP (Vucic et al., 2000; Kasof and Gomes, 2001), survivin (Conway et al., 2000; Shin et al., 2001), BRUCE (Bartke et al., 2004) and ILP2 (Richter et al., 2001; Lagace et al., 2001), have been reported to directly interact with and inhibit caspases, cysteine proteases that are the core components of the apoptotic cascade. The ectopic overexpression of these IAPs has been demonstrated to effectively inhibit apoptotic cell death triggered by various stimuli, including death receptor activation, withdrawal of growth factors, and exposure to cytotoxic insults (Deveraux and Reed, 1999; Verhagen et al., 2001). Among the IAPs, XIAP is the most potent modulator of apoptosis, and most well characterized in terms of its caspase-inhibitory activity. It

blocks cell death both *in vitro* and *in vivo* by inhibiting distinct caspases [Deveraux et al., 1997; Takahashi et al., 1998; Sun et al., 2000].

#### 1.1.4. HSP90 protein family:

HSP90 proteins take part in essential cellular processes and regulatory pathways like apoptosis, cell cycle control, cell viability, protein folding and degradation, and signalling events (Whitesell and Lindquist, 2005). Cancer cells exhibit a distinctive hallmark, which is relentless, uncontrolled cell division. They are marked by an absence of the inherent regulatory mechanisms that govern normal cell proliferation and maintain cellular balance (Miyata et al., 2013). Several cancer proteins depend on HSP90 machinery and chaperones for their folding and maturation (Vartholomaiou et al., 2016). members belonging to HSP90 protein family are molecular chaperones promoting the folding of de novo synthesized or incorrectly folded proteins, thus counteracting their aggregation (Chen et al., 2006). For instance; signalling kinases, steroid hormone receptors, and transcription factors, which are highly required in cancer development and progression, represent a group of HSP90 client proteins. These clients play various roles in the process of carcinogenesis, including uncontrolled proliferation, immortalization, anti-apoptotic functions, angiogenesis support, evasion of immune response, alterations in cellular energetics, genome instability, mutation induction, promotion of tumor-associated inflammation, escape from growth suppressors, and facilitation of invasion and metastasis. Consequently, the heightened sensitivity of cancer cells to HSP90 inhibitors, compared to healthy cells, has generated significant interest in the therapeutic realm of cancer treatment. (Abdullah et al, 2018).

#### 1.2. Molecular interaction:

The study of the interactions between receptors and drugs are important in pharmacology and clinical medicine and also in research and design of new compounds. The computational simulation by molecular docking procedure may be used to have more information about the specificity of the binding site and for the prediction of ligand-receptor interactions. The *in silico* method can be used as an alternative and complement to *in vitro* methods which may provide details of these molecular interactions. The studies by molecular docking are important, not only from a theoretical viewpoint, to explain the relationship between the structure of ligand and the function of protein but also in terms of practical applications, as they allow interpretation of the transporting process and therapeutic effectiveness of drugs.

#### 1.2.1. Types of interactions:

Hydrogen bonds are pivotal in shaping the specificity of ligand binding and upholding the three-dimensional structures of nucleic acids and proteins. Their significant influence is expressly integrated into a computational technique known as GRID, developed to identify energetically favorable ligand binding sites on a designated target molecule with a known structure. These bonds are well-recognized for their dominant role in preserving the three-dimensional configurations of both nucleic acids and proteins. Van-der waals (VDW)

interactions are short-range interactions, hence, play a major role in stabilizing protein–small molecule and DNA–small molecule complexes in biological processes. Because of the structural difference between the peptide and water, VDW interactions favour peptide intramolecular interactions and are a major contributing factor to the structural compactness. A sigma bond is a bond formed by the overlap of orbitals in an end-to-end fashion, with the electron density concentrated between the nuclei of the bonding atoms. A pi bond is a bond formed by the overlap of orbitals in a side-by-side fashion with the electron density concentrated above and below the plane of the nuclei of the bonding atoms. pi stacking or  $\pi$ - $\pi$  stacking refers to the non-covalent pi interactions (orbital overlap) between the pi bonds of aromatic rings. As direct stacking of aromatic rings (the "sandwich interaction") is electrostatically repulsive, therefore, the more commonly observed conformation is either a staggered stacking (parallel displaced) or pi-teeing (perpendicular T-shaped) interaction both of which are electrostatically attractive. These staggered stacking and  $\pi$ -teeing interactions between aromatic rings are important in nucleobase stacking

within DNA and RNA molecules, protein folding, template-directed synthesis, materials science, and molecular recognition (Lewis *et al.*, 2016; Martinez and Iverson, 2012). Offset parallel or perpendicular geometries were observed in a survey of high-resolution x-ray protein crystal structures in the Protein Data Bank (Huber *et al.*, 2014). The fundamental structure of an amide consists of a carbonyl group (C=O) bonded to a nitrogen atom (N) with a single bond, and the nitrogen atom is also bonded to two additional substituents, typically hydrogen atoms (H). The  $n \rightarrow \pi^*$  Amide interaction is widely present in the backbones of proteins and peptides 37–49 where the lone pair of electrons on the oxygen atom of a carbonyl group is delocalized into the  $\pi^*$  orbital of a neighbouring carbonyl group. In pi-alkyl interactions, there is interaction of pi- electron cloud over an aromatic group and electron group of any alkyl group. In pi-sulphur interaction, pi electron cloud of aromatic ring interacts with lone pair of electron cloud of sulphur atom. Cation- $\pi$  interaction is a noncovalent molecular interaction between the face of an electron-rich  $\pi$  system (e.g. benzene, ethylene, acetylene) and an adjacent cation (e.g.  $\text{Li}^+$ ,  $\text{Na}^+$ ). This interaction is an example of noncovalent bonding between a monopole (cation) and a quadrupole ( $\pi$  system). cation- $\pi$  interactions play an important role in nature, particularly in protein structure, molecular recognition, and enzyme catalysis (Dougherty and Ma, 1997).

In this study, the primary aim was to investigate potential novel drug lead candidates derived from TC, specifically for their potential in cancer treatment. The research involved screening phytoconstituents from TC against a panel of proteins frequently expressed in cancer cells. The research then delved into a detailed analysis of the binding energy and interactions between the phytoconstituents and the selected proteins, shedding light on their potential therapeutic properties.

## 2. MATERIALS AND METHODS:

From extensive literature search, a total of 33 reported compounds were selected and were listed out along with their Pub Chem IDs.

**Table 1: List of ligands (phytochemical compounds) reported from literature:**

Sl. Nos.	Ligands	PUB-CHEM ID
1	Aporphine	114911
2	Berberine	2353
3	$\beta$ - sitosterol	222284
4	Chasmanthin	442012
5	Choline	305
6	Columbin	188289
7	Cordifoline	21593932
8	Cordioside	101915817
9	Clerodane	11969563
10	Ecdysterone	5459840
11	Gamma Sitosterol	457801
12	Isocorydin	10143
13	Jatrorrhizine	72323
14	Magnoflorine	73337
15	Makisterone A	12312690
16	Menisperine	161487
17	Norcoclaurine	114840
18	Oblongine	173713
19	Palmarin	442068
20	Palmatine	19009
21	Palmatoside G	184515
22	Pregnane	6857422
23	Pyrrolidone	12025
24	Reticulin	10233
25	Tembetarine	167718
26	Tetrahydropalmatine	5417
27	Tinocordifolin	100926540
28	Tinocordifolioside	100926541
29	Tinocordioside	101916313
30	Tinosponone	15215479
31	Tinosporaside	14194109

32	Yangambin	443028
33	Syringin	5316860

During cancer, few receptors are commonly expressed on the cancer cells. They are listed below.

**Table 2: List of receptors that are expressed during cancer:**

Receptor pdb code	Brief description
2O22	Solution structure of the anti-apoptotic protein Bcl-2 in complex with an acyl-sulfonamide-based ligand
4AUQ	Structure of BIRC7-UbcH5b-Ub complex
1XBO	Structure of the BIR domain of IAP-like protein 2
4L8Z	Crystal structure of Human Hsp90 with RL1

### 2.1. Ligand preparation

The molecular structures of phytoconstituents sourced from TC were initially obtained from the PubChem database (<https://pubchem.ncbi.nlm.nih.gov/>) and cross-verified using the ChemSpider database (<http://www.chemspider.com/>). Subsequently, these compounds were converted into a suitable format, mol2, for further analysis. The energy-minimized structures were utilized in subsequent docking studies.

### 2.2. Receptor preparation

To obtain the three-dimensional crystal structures of the receptors, we accessed the Protein Data Bank (PDB) at <http://www.rcsb.org/pdb/>. Subsequently, for the proteins, we assigned missing bonds, bond orders, explicit hydrogen, charges (calculated via Molegro Virtual Docker), and flexible torsion using the 'Protein Preparation' module within Molegro Virtual Docker. The receptor's chemical properties were adjusted to ensure the correct protonation states, while any crystallographic water molecules associated with the protein were eliminated.

### 2.3. Lipinski's rule of five

For a molecule to qualify as a potential drug, it must adhere to Lipinski's Rule of Five, a set of criteria that predicts favorable drug-like properties. These criteria include (i) having no more than 5 hydrogen bond donors, (ii) a molecular weight below 500, (iii) a Log P (partition coefficient) less than 5, and (iv) having no more than 10 hydrogen bond acceptors. It's worth noting that certain compound classes that serve as substrates for biological transporters can be exceptions to these rules. In our study, we focused on commonly identified phytochemicals present in TC. These compounds were subsequently subjected to molecular docking with the aforementioned well-known four receptors, and an analysis was performed to assess their adherence to Lipinski's Rule of Five, which is a critical factor in evaluating their drug-like potential.

### 2.4. Molecular docking

Molecular docking was performed using the Molegro Virtual Docker (MVD) program. The 3D structure of the desired receptor protein molecule (already downloaded from RCSB PDB) was opened in MVD. While importing the pdb format of receptor protein, only the protein, its associated chains (all if different or a single copy if there are multiple copies of the same chain), and reference ligands (if any) were imported, leaving behind Cofactors (if any) and water molecules (if any). Then the mol2 formats of targeted ligands (already downloaded from PubChem) were imported to the workspace and optimized using protein preparation. The identification of the cavity with the potential binding site for ligands in the crystal structure was performed automatically using the grid-based cavity prediction algorithm. The residues close to cavity were minimized. For each complex, 10 independent runs were conducted, each of these runs was returning to a single final solution (pose). The resulting conformations were clustered and only the negative lowest-energy representation from each cluster was returned when the docking run was completed. The similar poses were removed keeping the best-scoring one. The cluster of ten poses was sorted in order of the MolDock Score. In order to increase the accuracy of the ranked order of the poses, the weighted reranking scores (Rerank Score) were used to evaluate the poses. For analysis, one pose with the lowest value of Rerank Score was selected as the best solution for each complex. The re-ranking score function is estimated more expensive than the scoring function used during the docking simulation, but it is commonly better than the docking score function at analyzing the best pose among several poses originating from the same ligand.

### 2.5. 2D and 3D visualisation:

Docking in MVD was followed by visualizing the interactions between ligands and receptors in Discovery Studio. Most drugs bind with the amino acids of target binding site in a reversible manner by means of weak chemical bonds. The several types of intermolecular bonding interaction such as hydrophobic, electrostatic, ionic, and hydrogen bonds differ in their bond strengths. The number and types of these interactions depend on the structure of the drug and functional groups that are present in the drug. 3D and 2D structures of the interaction are observed and analyzed for better understanding.

### 2.6. Docking of Bio-active compound:

Gas chromatography and mass spectroscopy (GCMS) of methanolic crude extract of TC yielded the presence of a bio-active compound namely Neotigogenin which was also subjected to docking along with the other reported phytochemical compounds in order to see the comparative affinity towards the receptors.

**Table 3: Name of ligand reported from isolation of crude extract of TC:**

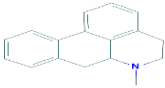
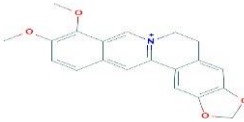
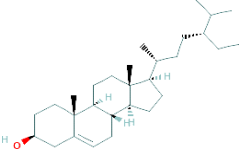
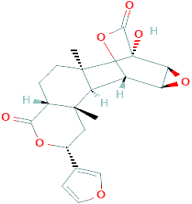
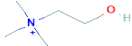
Sl. Nos.	Ligand	PUB-CHEM ID

1	Neotigogenin	12304433
---	--------------	----------

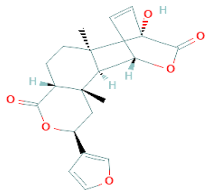
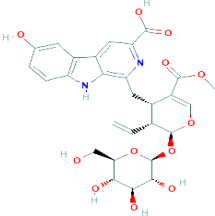
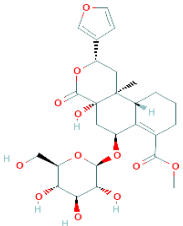
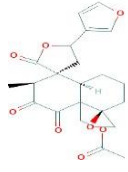
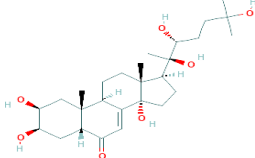
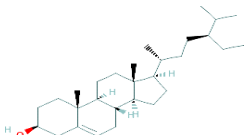
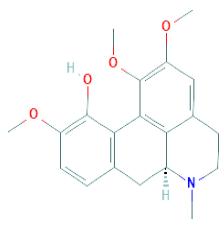
The docking was carried out altogether. The docking results were produced in both 3D and 2D poses. The data output was collected and produced in tabular form.

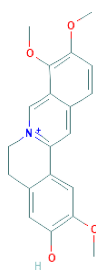
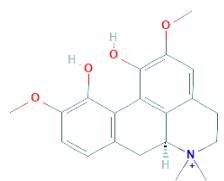
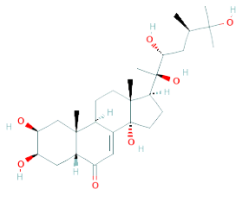
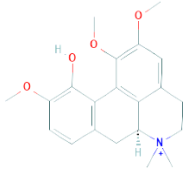
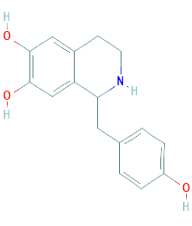
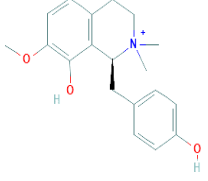
### 3. RESULTS:

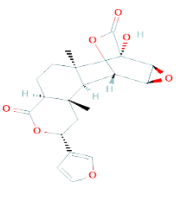
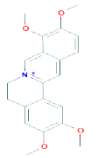
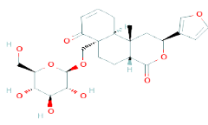
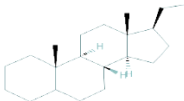
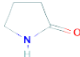
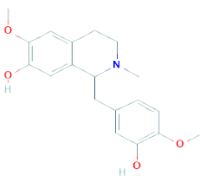
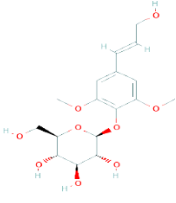
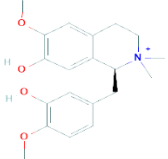
**Table 4: List of phytoconstituents collected from literature representing their 2D structure, PUB-CHEM ID, and Lipinski's rule of 5:**

Sl. No s.	Ligands	Structure	PUB-CHEM ID	Lipinski's Rule of 5				
				MW	Log p	HBD	HBA	NRB
1	Aporphine		114911	235.32	3	0	1	0
2	Berberine		2353	336.4	3.6	0	4	2
3	$\beta$ - sitosterol		222284	414.7	9.3	1	1	6
4	Chasmanthin		442012	374.4	1.3	1	7	1
5	Choline		305	104.17	-0.4	1	1	2

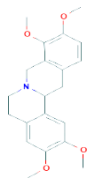

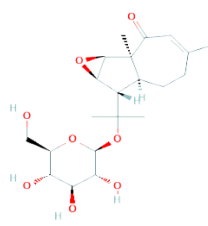
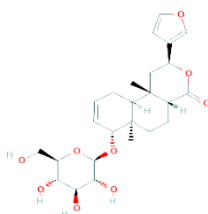
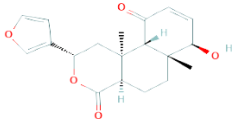
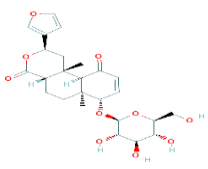
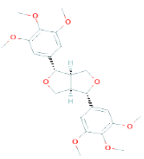


6	Columbin		188289	358.4	2.2	1	6	1
7	Cordifoline		21593932	586.5	0.8	7	13	9
8	Cordioside		101915817	538.5	-0.5	5	12	6
9	Clerodane		11969563	416.4	0.8	0	8	4
10	Ecdysterone		5459840	480.6	0.5	6	7	5
11	Gamma Sitosterol		457801	414.7	9.3	1	1	6
12	Isocorydine		10143	341.4	2.6	1	5	3

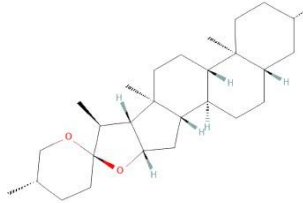
13	Jatrorrhizine		72323	338.4	3.4	1	4	3
14	Magnoflorine		73337	342.4	2.7	2	4	2
15	Makisterone A		12312690	494.7	0.9	6	7	5
16	Menisperine		161487	356.4	3.1	1	4	3
17	Norcoclaurine		114840	271.31	2.2	4	4	2
18	Oblongine		173713	314.4	3.1	2	3	3

19	Palmarin		442068	374.4	1.3	1	7	1
20	Palmatine		19009	352.4	3.7	0	4	4
21	Palmatoside G		184515	492.5	0.1	4	10	5
22	Pregnane		6857422	288.5	8.4	0	0	1
23	Pyrrolidone		12025	85.1	-0.8	1	1	0
24	Reticulin		10233	329.4	3	2	5	4
25	Syringin		5316860	372.4	-1.3	5	9	7
26	Tembetarine		167718	344.4	3	2	4	4



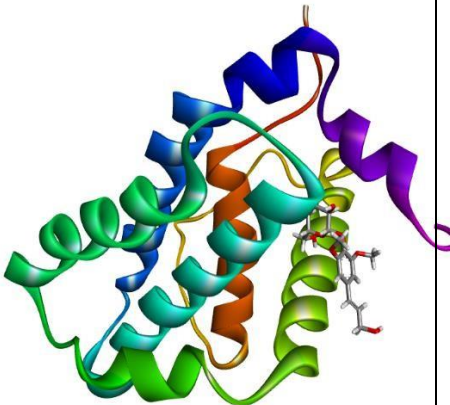
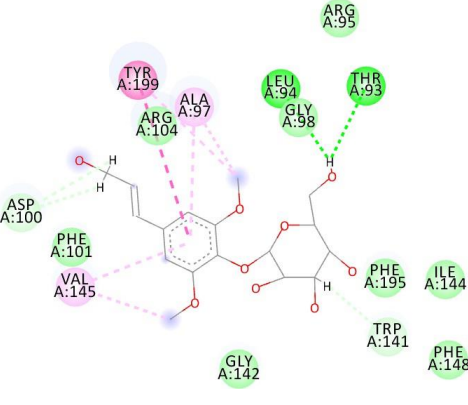
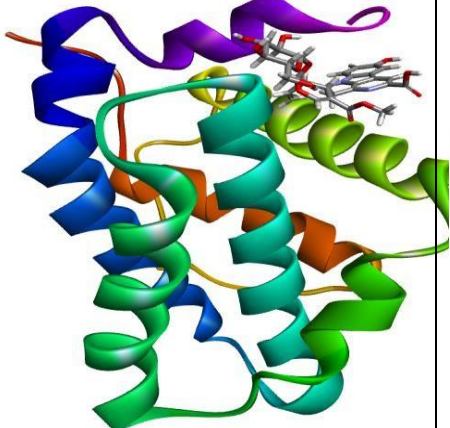
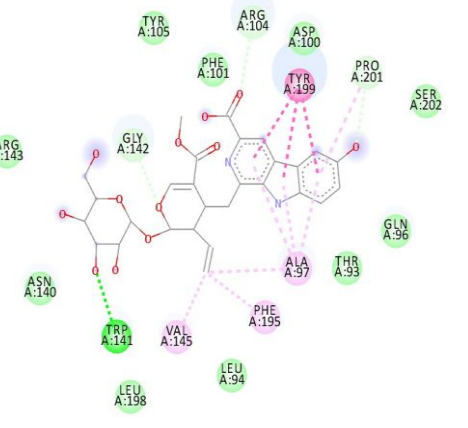
27	Tetrahydropal matine		5417	355.4	3.2	0	5	4
28	Tinocordifolin		100926540	250.33	1.4	1	3	1
29	Tinocordifolios ide		100926541	412.5	-0.2	4	8	4
30	Tinocordioside		101916313	478.5	1.3	4	9	4
31	Tinosponone		15215479	330.4	1.8	1	5	1
32	Tinosporaside		14194109	492.5	0.2	4	10	4
33	Yangambin		443028	446.5	2.9	0	8	8

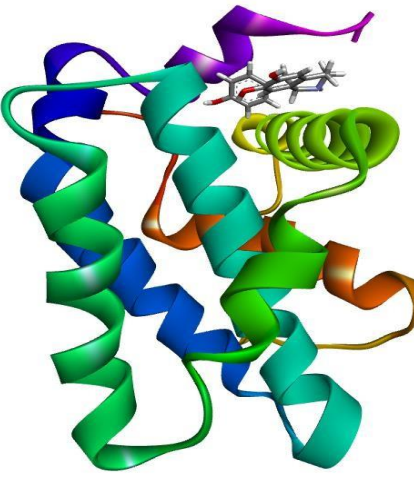
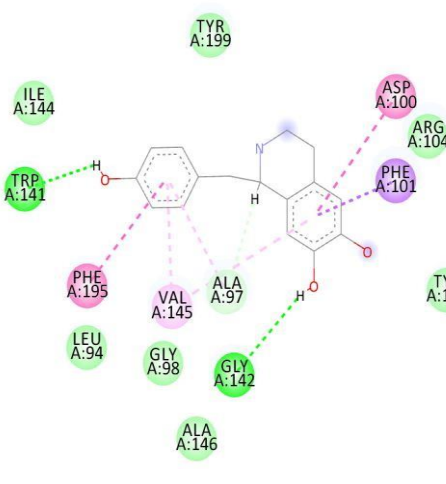
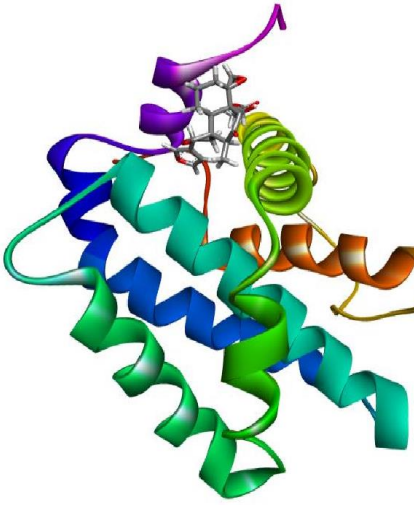
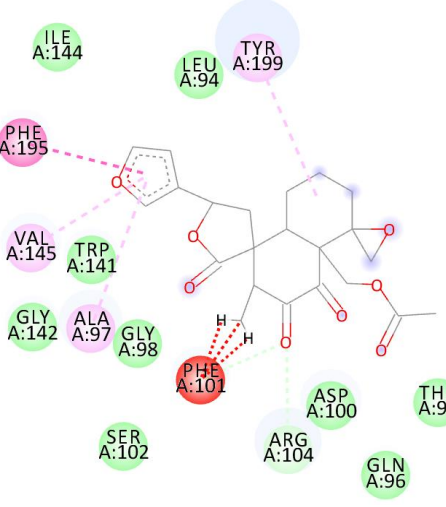
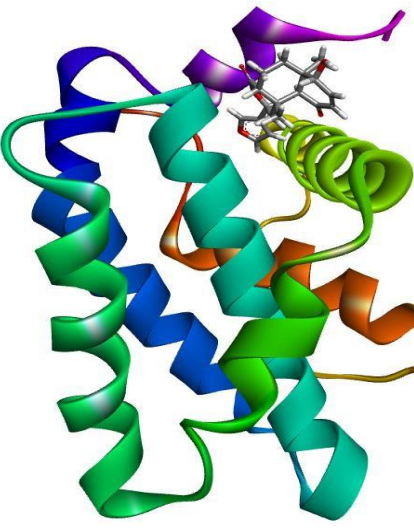
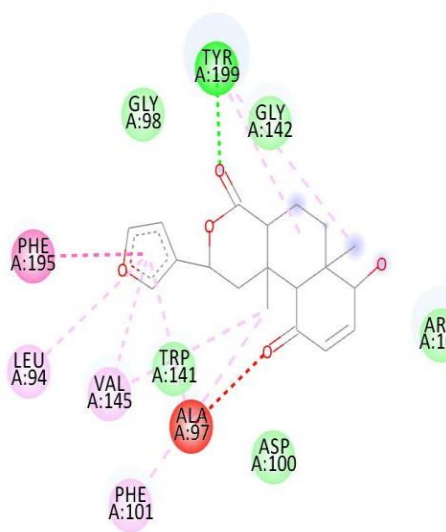
**Table 5: Bio-active compound representing its 2D structure, PUB-CHEM ID, and Lipinski's rule of 5**

Sl. Nos	Ligands	Structure	PUB-CHEM ID	Lipinski's Rule of 5				
				MW (g/mol)	Log p	HBD	HBA	NRB
1	Neotigogenin		1230443	416.6	6.5	1	3	9

**3.1. Molecular docking of compounds of TC with anti-apoptotic receptors:**

**3.1.1. Anti-apoptotic protein Bcl-2 in complex with an acyl-sulfonamide-based ligand (PDB CODE: 2O22)**

Name of the Ligand	3D - structure	2D - structure
1) Syringin		
2) Cordifolin		

<p>3) Norcoclaurin</p>		
<p>4) Clerodane</p>		
<p>5) Tinosponon</p>		

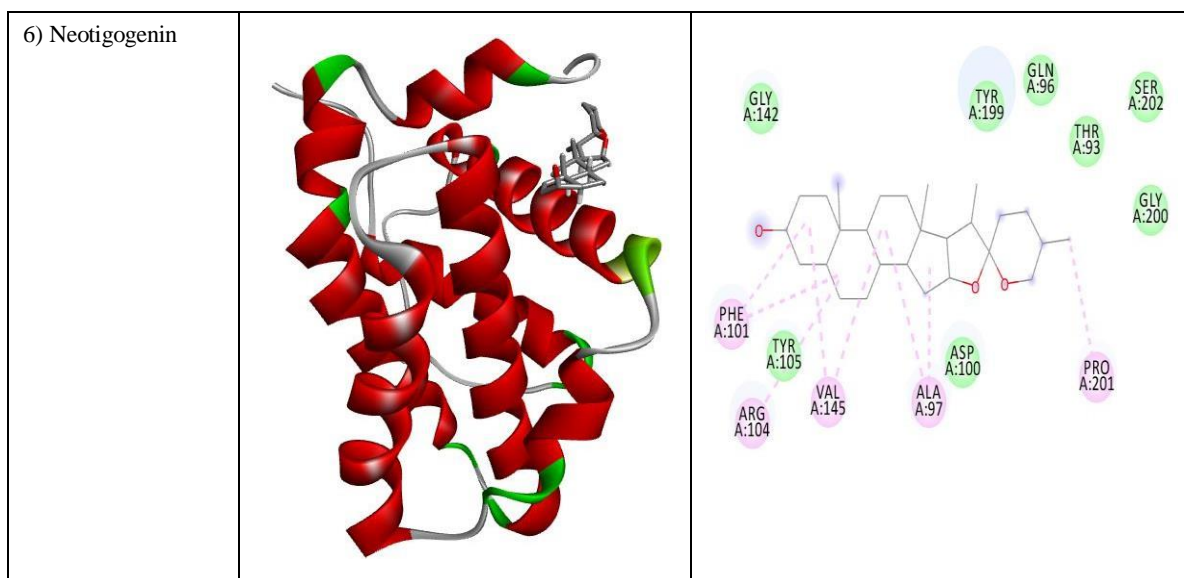
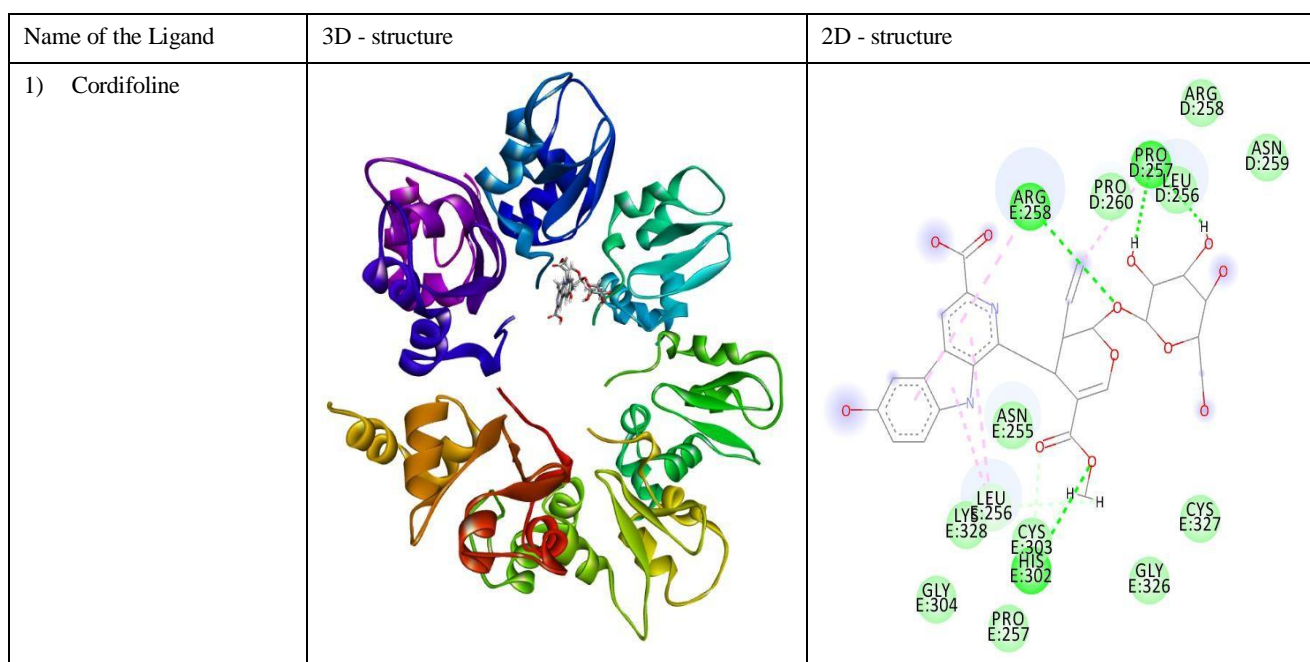


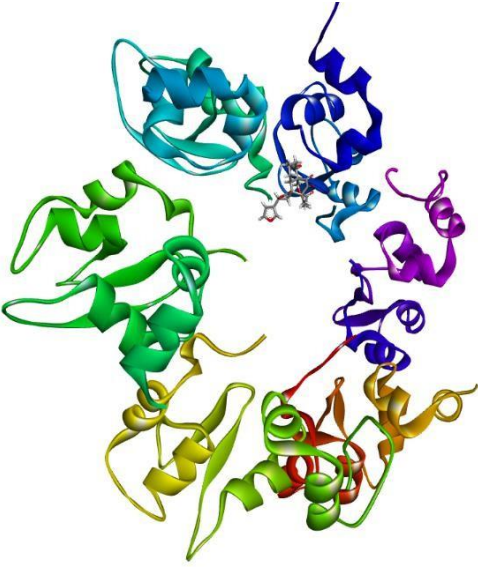
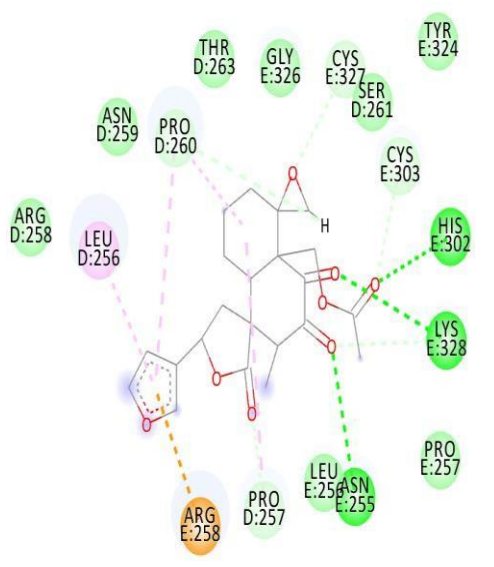

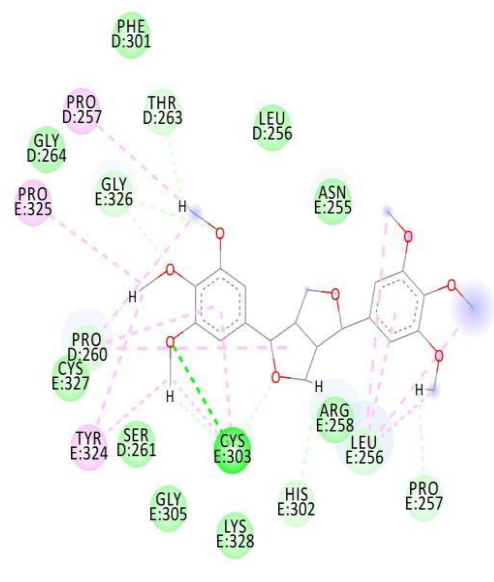
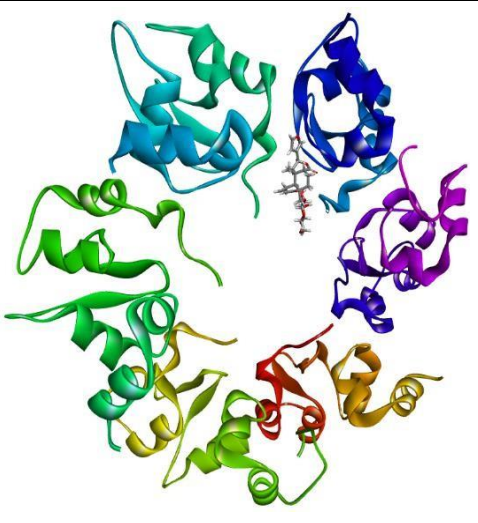
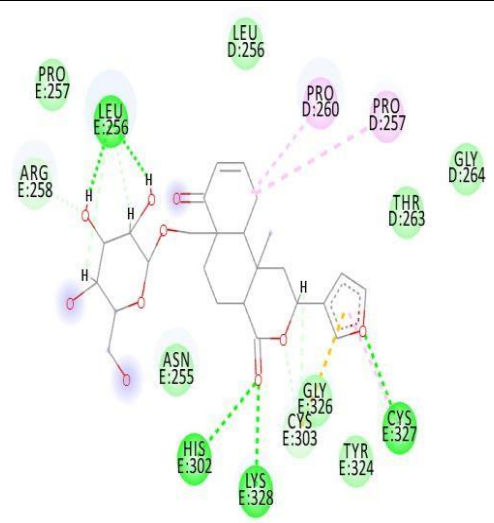
Figure 1: 3D and 2D structures of receptor 2022 showing ligand-receptor interaction arranged on the basis of highest negative average rerank score

- Conventional hydrogen bond ●
- Van-der waals interaction ●
- Carbon hydrogen bond ●
- Pi – pi stacked/amide-pi stacked ●
- Pi alkyl bond /alkyl bond ●
- Pi sigma bond ●
- Pi-anionic/pi-cationic ●
- Unfavorable bump ●

### 3.1.2. Structure of the BIR domain of IAP-like protein 2 (PDB CODE – 1XB0)





<p>2) Clerodane</p>		 <p>Residues involved in interactions: THR D:263, GLY E:326, CYS E:327, SER D:261, TYR E:324, ASN D:259, PRO D:260, ARG D:258, LEU D:256, ARG E:258, PRO D:257, LEU E:255, ASN E:255, LEU E:256, CYS E:303, HIS E:302, LYS E:328, PRO E:257.</p>
<p>3) Yangambin</p>		 <p>Residues involved in interactions: PHE D:301, PRO D:257, THR D:263, LEU D:256, GLY D:264, PRO E:325, GLY E:326, ASN E:255, PRO D:260, CYS E:327, TYR E:324, SER D:261, CYS E:303, ARG E:258, LEU E:256, GLY E:305, LYS E:328, HIS E:302, PRO E:257.</p>
<p>4) Palmatoside G</p>		 <p>Residues involved in interactions: LEU D:256, PRO E:257, ARG E:258, ASN E:255, HIS E:302, LYS E:328, GLY E:326, CYS E:303, TYR E:324, CYS E:327, PRO D:260, PRO D:257, THR D:263, GLY D:264.</p>

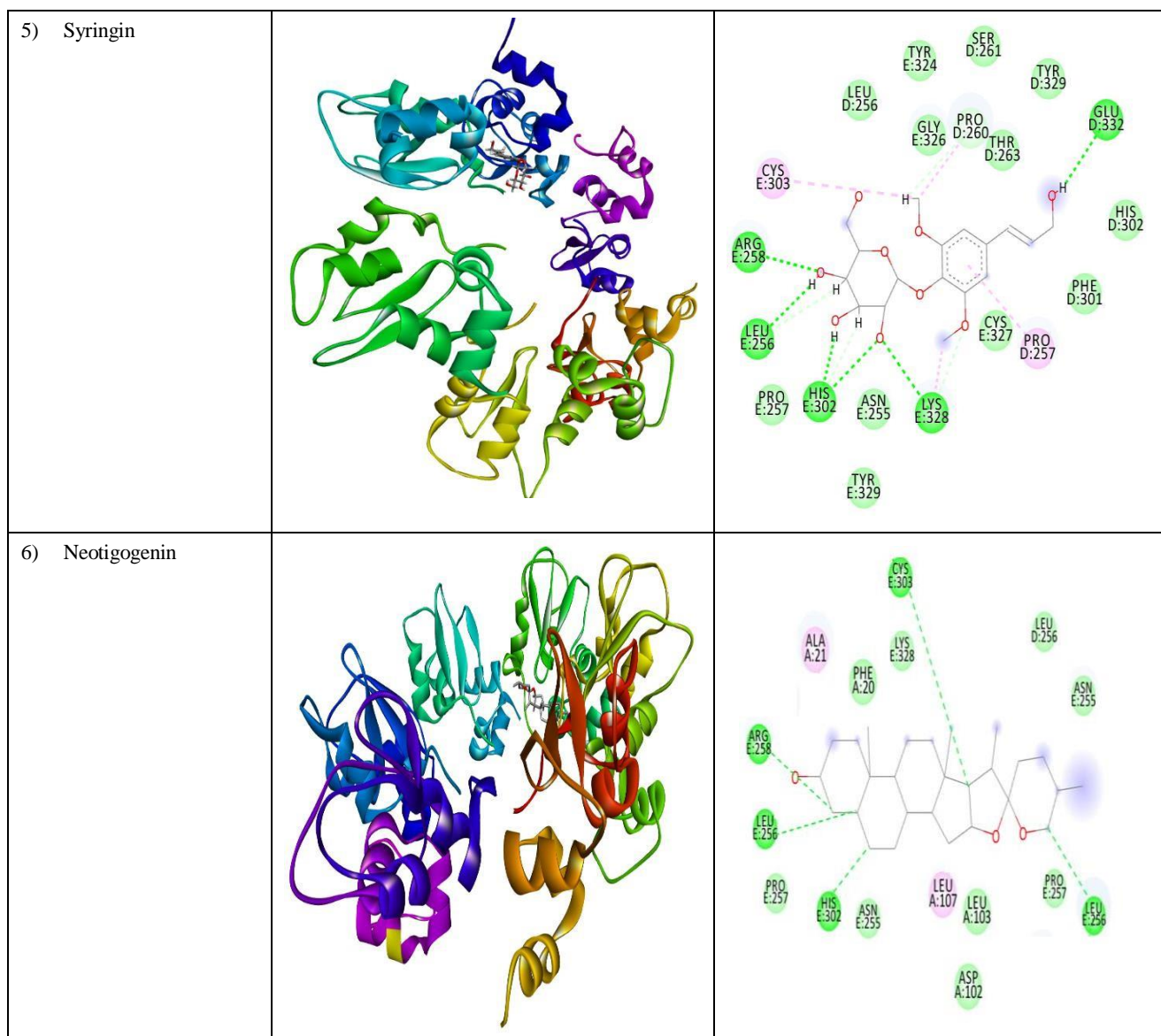









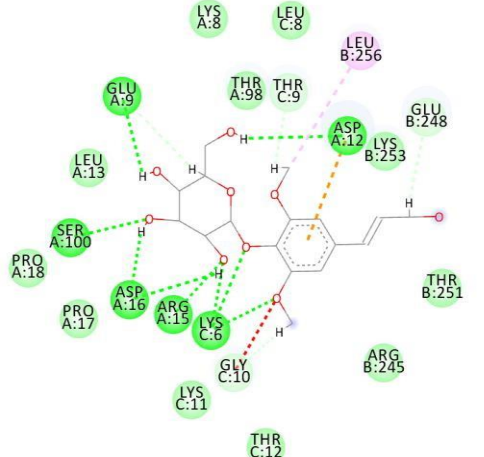

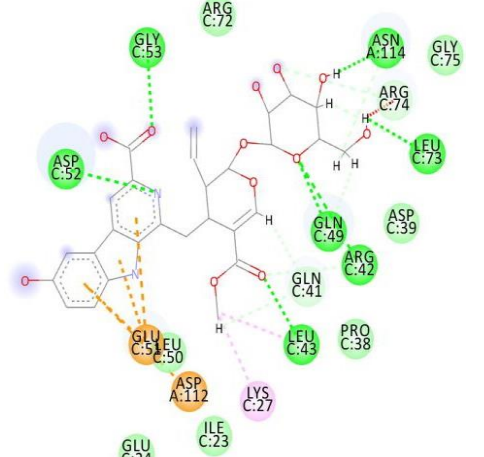
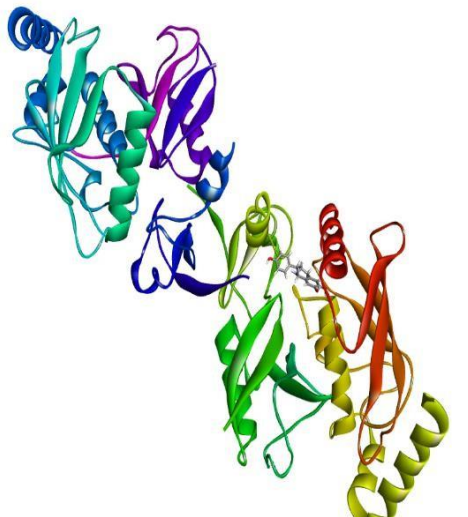
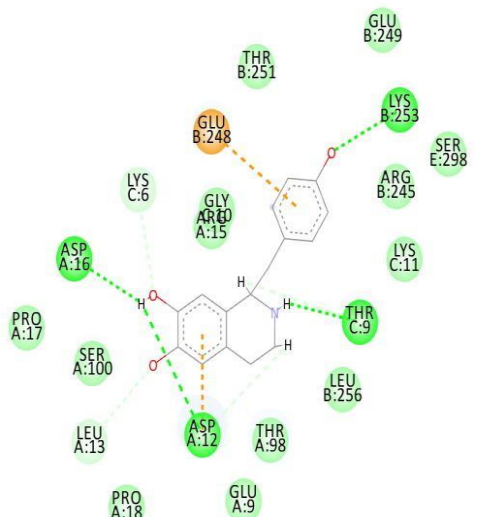


Figure 2: 3D and 2D structures of 1XB0 showing ligand-receptor interaction arranged on the basis of highest negative average rerank score

Conventional hydrogen bond	
Van-der waals interaction	
Carbon hydrogen bond	
Pi – pi stacked/amide-pi stacked	
Pi alkyl bond /alkyl bond	
Pi sigma bond	
Pi-anionic/pi-cationic	
Unfavorable bump	

3.1.3. Structure of BIRC7-UbcH5b-Ub complex (PDB CODE – 4AUQ)

Name of the Ligand	3D - structure	2D - structure
1) Syringin		
2) Cordifolin		
3) Norcochlorine		



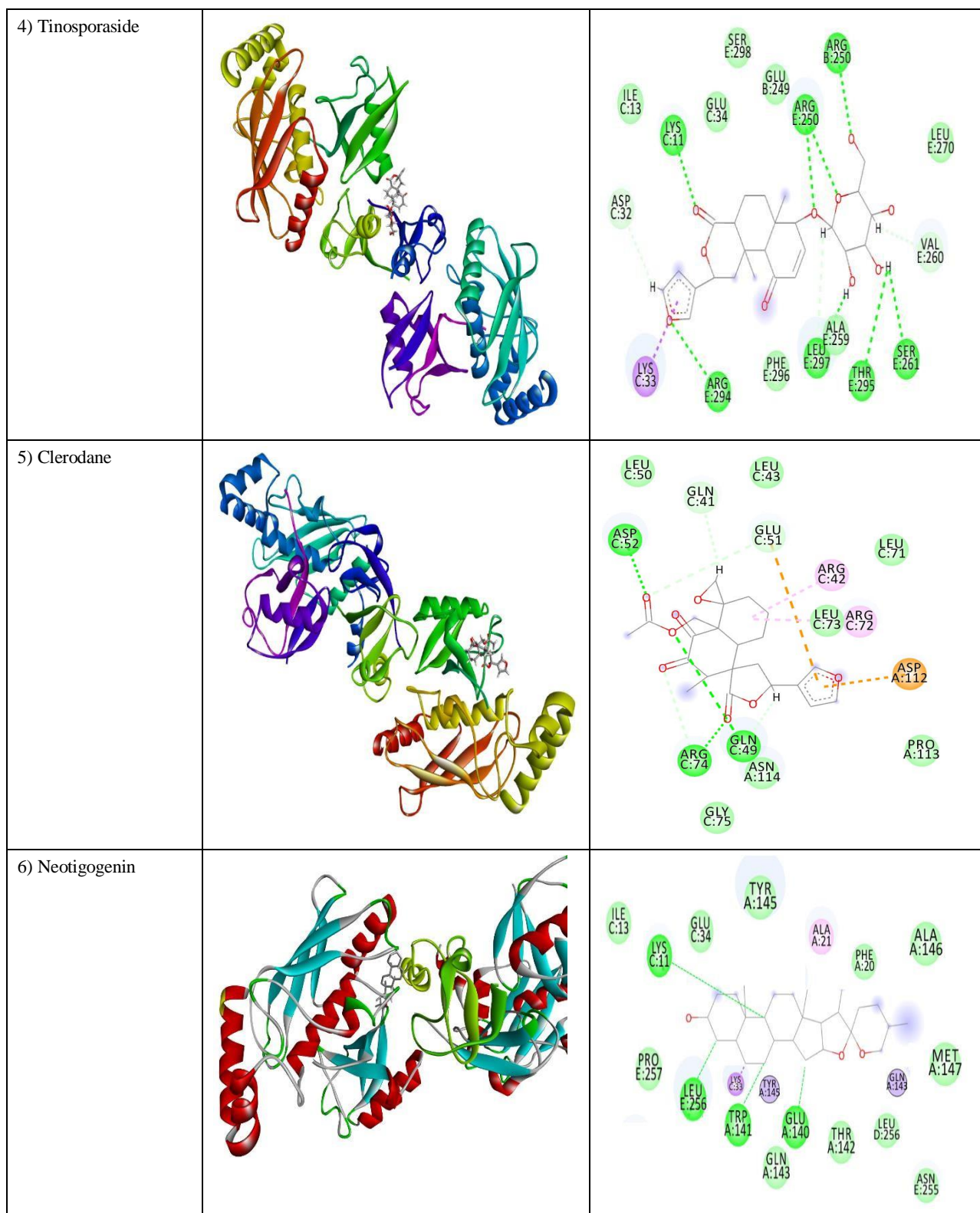
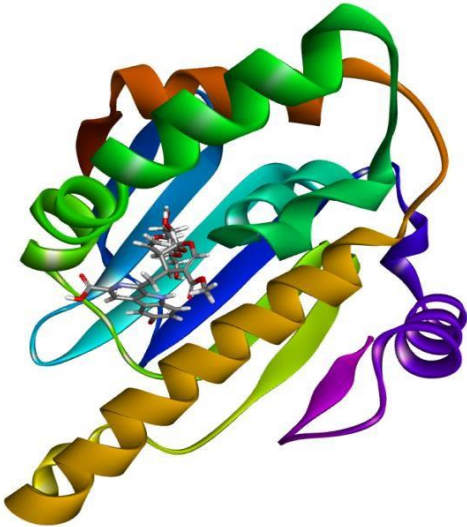
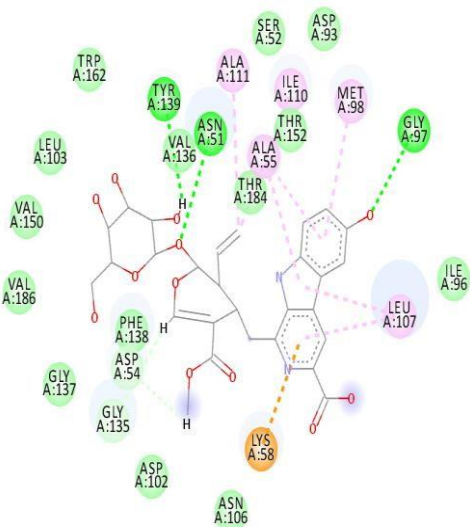
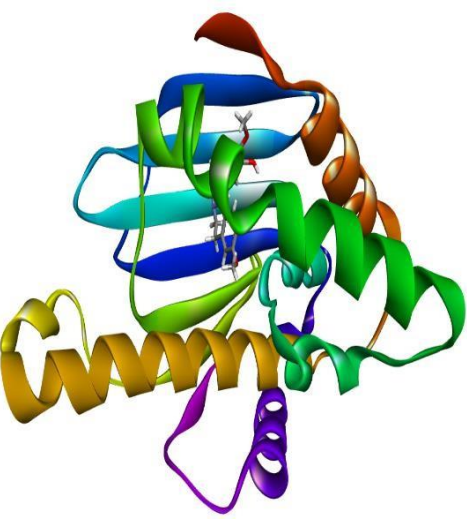
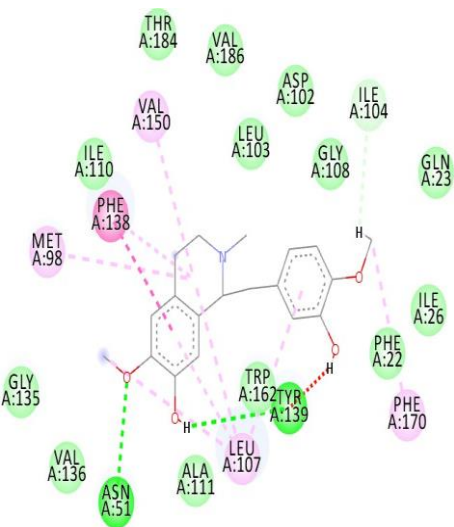


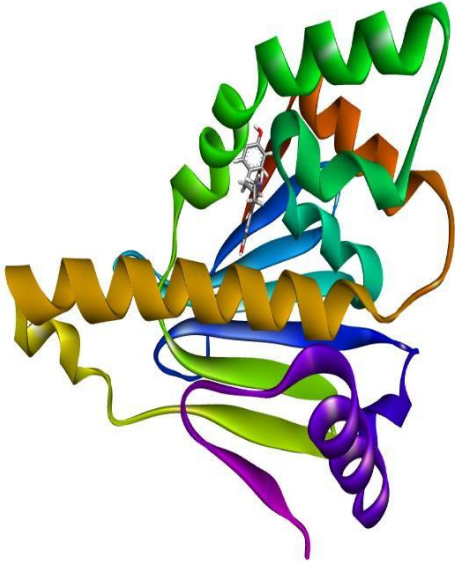
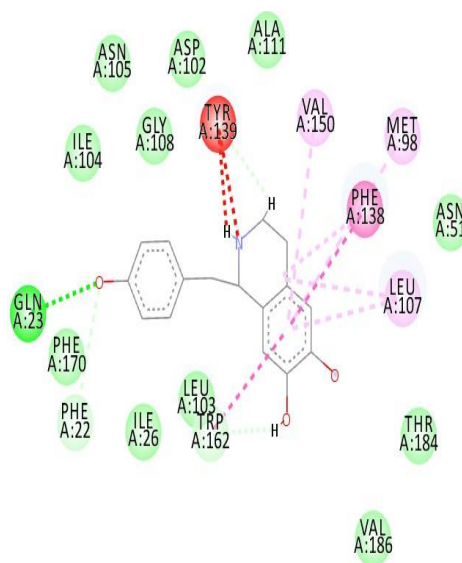
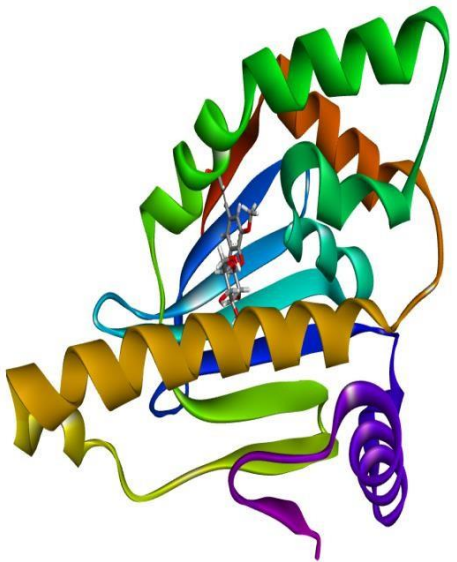
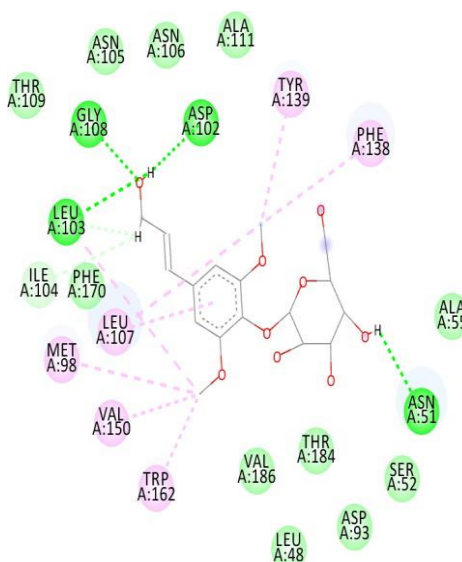
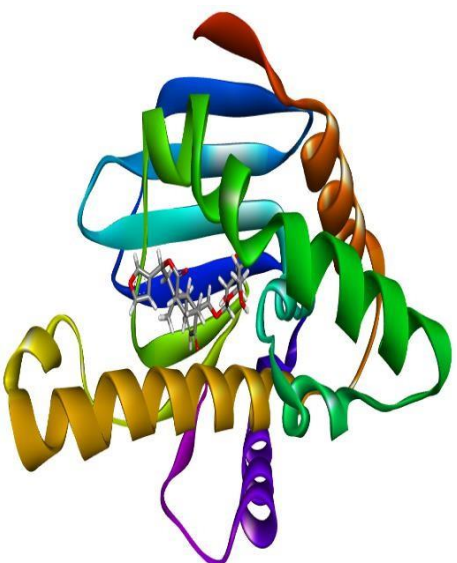
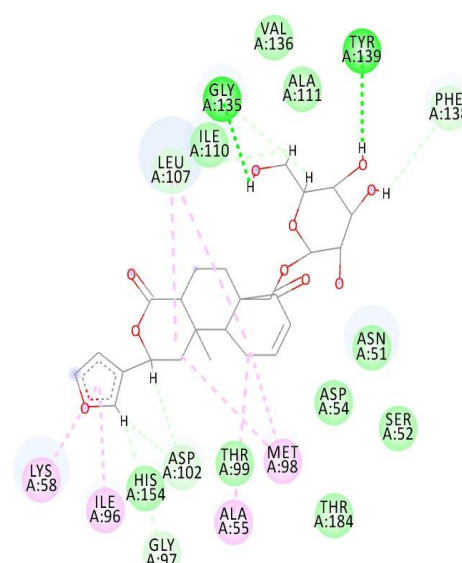
Figure 3: 3D and 2D structures receptor 4AUQ showing ligand-receptor interaction arranged on the basis of highest negative average rerank score

Conventional hydrogen bond ●  
 Van-der waals interaction ●  
 Carbon hydrogen bond ●  
 Pi – pi stacked/amide-pi stacked ●

- Pi alkyl bond /alkyl bond
- Pi sigma bond
- Pi-anionic/pi-cationic
- Unfavorable bump

3.1.4. HSP90 protein structure (PDB CODE – 4L8Z)

Name of the Ligand	3D - structure	2D - structure
1) Cordifoline		
2) Reticulin		

<p>3) Norcochlorine</p>		
<p>4) Syringin</p>		
<p>5) Palmatoside G</p>		



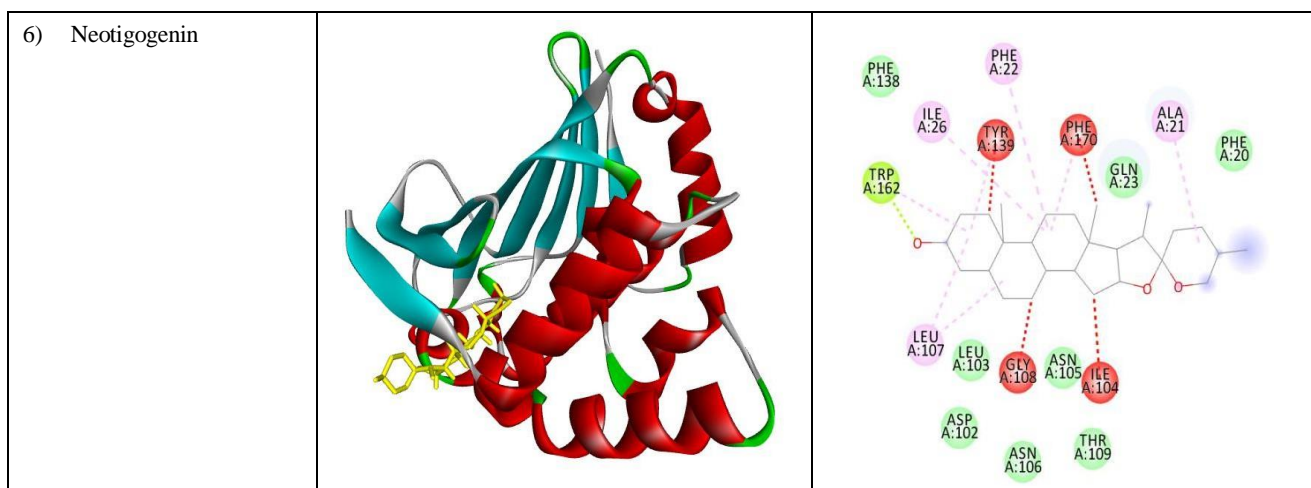


Figure 4: 3D and 2D structures of 4L8Z showing ligand-receptor interaction with receptor 4L8Z arranged on the basis of highest negative average rerank score.

- Conventional hydrogen bond ●
- Van-der waals interaction ●
- Carbon hydrogen bond ●
- Pi – pi stacked/amide-pi stacked ●
- Pi alkyl bond /alkyl bond ●
- Pi sigma bond ●
- Pi-anionic/pi-cationic ●
- Unfavorable bump ●

Table 6: Evaluation of H-bond energy in receptor-ligand binding

Ligands	Mol dock score	Re rank score	H-bond energy	Number of interactions
Receptor: Bcl-2 (PDB ID: 2O22)				
Norocclaurin (114840)	-100.648	-74.47986	-3.59741	14
Syringin (5316860)	-124.796	-80.58398	-2.26607	15
Clerodane (11969563)	-111.478	-74.16164	-2.23813	15
Tinosponon (15215479)	-108.417	-71.90304	-0.959522	11
Cordifoline (21593932)	-154.608	-77.7005	-4.34893	18
Neotigogenin (12304433)	-124.596	-83.6096	-0.737498	13
Receptor: ILP2 (PDB ID: 1XB0)				
Palmatoside G (184515)	-131.038	-75.98588	-7.9893	15
Yangambin (443028)	-117.293	-76.42248	-1.64833	19
Syringin (5316860)	-114.028	-75.88692	-13.5792	20
Clerodane (11969563)	-129.127	-83.54414	-4.05649	17
Cordifoline (21593932)	-148.012	-86.39696	-12.3936	15
Neotigogenin (12304433)	-108.185	-78.6038	-9.40219	16

Receptor: (PDB ID: 4AUQ)				
Norcoclaurine (114840)	-105.931	-77.70972	-7.20859	20
Syringin (5316860)	-120.346	-85.35098	-17.0824	21
Clerodane (11969563)	-113.978	-67.26466	-6.06109	15
Tinosporaside (14194109)	-116.511	-69.50004	-13.2488	17
Cordifoline (21593932)	-154.518	-80.09038	-7.25395	19
Neotigogenin (12304433)	-122.184	-77.8386	-7.66463	19
Receptor: HSP 90 (PDB ID: 4L8Z)				
Reticulin (10233)	-128.208	-89.25922	-3.22668	21
Norcoclaurine (114840)	-106.816	-81.95496	-3.60615	19
Palmatoside G (184515)	-120.462	-76.89596	-3.71568	19
Syringin (5316860)	-125.236	-78.34792	-4.84444	22
Cordifoline (21593932)	-166.966	-115.856	-6.55348	25
Neotigogenin (12304433)	-116.446	-75.5293	-0.39547	17

From the above-presented data, it can be said that, in receptor 2O22, the highest hydrogen bond energy was exhibited by cordifoline (-4.34893 kJ/mol) followed by Norcoclaurine (-3.59741 kJ/mol) and syringin (-2.26607 kJ/mol). Cordifoline was found to establish only one hydrogen bond, 10 van der Waals interactions, 3 carbon-hydrogen bonds, 1 pi-pi stacked, 1 pi alkyl, and 2 alkyl bonds. Norcoclaurine showed 2 hydrogen bond interactions, 7 van der Waals interactions, 1 carbon-hydrogen bond, 1 pi-pi stacked, 1 pi alkyl and 1 amide – pi stacked, and 1 pi-sigma bond interaction. While syringin was also able to establish 2 hydrogen bonds, 8 van der Waals interactions, 2 carbon-hydrogen bonds, 1 pi-pi stacked, 1 pi alkyl, and 1 alkyl bond. Therefore, it can be evaluated that syringin and norcoclaurine bind to the receptor in sites which are more energetically favourable than cordifoline. Cordifoline with 10 van der Waal interaction shows more structural stability than syringin with 8 and norcoclaurine with 7 interactions respectively. Presence of 3 C-H bonds in case of cordifoline makes it more stable than syringin with 2 and norcoclaurine with 1 C-H bond respectively. Presence of 1 pi-pi stacked bond in all three ligand-receptor interactions mean that there is a non-covalent pi interaction (orbital overlap) between the pi bonds of aromatic rings. Similarly, presence of 1 pi-alkyl bond in all three ligand receptor interactions mean that there is interaction of pi- electron cloud over an aromatic group and electron group of an alkyl group. Presence of 1 amide-pi bond in case of norcoclaurine mean that the lone pair of electrons on the nitrogen atom of an amide group is delocalized into the  $\pi^*$  orbital of a neighbouring amide group and 1 sigma bond implies that there is a sidewise overlap of orbitals between the ligand and the receptor. Presence of 2 alkyl groups in cordifoline makes it more potent than syringin with 1 alkyl group. Overall, cordifoline becomes the best fit out of the top three ligands in establishing a more stable interaction with the receptor. Thus, cordifoline exhibits the highest potential to bind to the anti-apoptotic receptor 2O22

and in turn inhibit it so that the protein gets downregulated in cancer cells leading to apoptosis.

Similarly, in receptor 1XB0, the highest hydrogen bond energy was exhibited by syringin (-13.5792 kJ/mol) followed by cordifoline (-12.3936 kJ/mol) and neotigogenin (-9.40219 kJ/mol). Syringin was found to establish 5 conventional hydrogen bonds, 12 van der Waals interactions, 1 carbon-hydrogen bond, 1 pi alkyl, and 1 alkyl bond respectively. Cordifoline showed 3 hydrogen bond interactions, 11 van der Waals interactions, and 1 carbon hydrogen bond interaction. While neotigogenin was able to establish 5 hydrogen bonds, 9 van der Waals interactions, and 2 alkyl bonds. Therefore, it can be evaluated that syringin and neotigogenin respectively bind to the receptor in sites which are more energetically favourable than cordifoline. Syringin with 12 van der Waals interaction shows more structural stability than neotigogenin and cordifoline each with 11 interactions respectively. While, presence of only 1 C-H bond in both the cases of syringin and cordifoline respectively makes it a little difficult to compare the stability of the conformation. Presence of 1 pi-alkyl bond and 1 alkyl bond in syringin and 1 alkyl bond interaction in neotigogenin indicate that there is interaction of pi-electron cloud over an aromatic group and electron group of an alkyl group which makes them more potent than cordifoline with no such non-covalent interactions at all. Overall, syringin is found to score more in producing a more energetically favourable interaction followed by neotigogenin and cordifoline. Thus, syringin exhibits the highest potential to bind to the anti-apoptotic receptor 1X0X and in turn inhibit it so that the protein gets downregulated in cancer cells leading to cell death.

In receptor 4AUQ, the highest hydrogen bond energy was exhibited by syringin (-17.0824 kJ/mol) followed by tinosporaside (-13.2488 kJ/mol) and neotigogenin (-7.66463 kJ/mol). Syringin was found to establish 6 conventional hydrogen bonds, 11 van der Waals interactions, 3 carbon-

hydrogen bond, 1 pi anionic bond, and 1 alkyl bond respectively. Tinosporaside showed 7 hydrogen bond interactions, 7 van der Waals interactions, 2 carbon-hydrogen bond interaction, and 1 pi-sigma bond interaction. While neotigogenin was able to establish 4 hydrogen bonds, 11 van der Waals interactions, 1 alkyl bond, and 2 covalent interactions. Syringin with 6 H-bonds implies that the stability is slightly less when compared to tinosporaside with 7 H-bonds. While 11 van der Waals interactions between ligand and receptor in case of syringin and neotigogenin each respectively establishes more structural compactness than tinosporaside with 7 interactions. Presence of 3 C-H bonds in syringin makes the ligand more energetically favourable than the other two ligands. Presence of 1 pi-anionic bond in case of syringin indicate interaction between an electron-rich pi-system and an adjacent anion which holds a major importance in protein structure maintenance. But, presence of 1 alkyl bond both in case of syringin and neotigogenin each respectively make them more potent of making a strong interaction with the receptor. Presence of 1 pi-sigma bond in case of tinosporaside indicate that there is a side-wise overlap between s and p orbitals of the adjacent atoms. Therefore, it can be deduced that syringin binds to the receptor in sites which are more energetically favourable than neotigogenin and tinosporaside respectively. Thus, syringin exhibits the highest potential to bind to the receptor 4AUQ and in turn inhibit it so that the family of ubiquitin ligase gets downregulated in cancer cells and in turn the tumour suppressors don't get inactivated by any factors which will lead to tumour cell death.

In receptor 4L8Z, the highest hydrogen bond energy was exhibited by cordifoline (-6.55348 kJ/mol) followed by syringin (-4.84444kJ/mol) and palmatoside G (-3.71568 kJ/mol). Cordifoline was found to establish 3 conventional hydrogen bonds, 14 van der Waals interactions, 2 carbon-hydrogen bond, 1 pi-cationic bond, 3 pi-alkyl bonds, and 2 alkyl bonds respectively. Syringin showed 4 hydrogen bond interactions, 11 van der Waals interactions, 1 carbon-hydrogen bond interaction, and 1 pi-alkyl and 5 alkyl bond interactions. While palmatoside G was only able to establish 2 hydrogen bonds, 9 van der Waals interactions, 3 carbon hydrogen bonds, 1 pi-donor hydrogen bond, 2 pi-alkyl, and 2 alkyl bond. Therefore, syringin with 4 H-bonds account for more stability in comparison to cordifoline with 3 and palmatoside G with 2 conventional H-bonds respectively. While, in terms of van der Waals interaction, the lead position has to be given to cordifoline with 14 interactions followed by syringin with 11 and palmatoside G with 9 interactions respectively i.e., cordifoline exhibits more structural compactness with the receptor than the other two ligands. The 3 C-H bonds in case of palmatoside G makes it stronger amongst the other two ligands in establishing stronger co-valent interactions than the other two ligands. Presence of a total of 6 non-covalent interactions in case of syringin makes it more potent with a total of 5 alkyl bonds and 1 pi-alkyl bond in comparison to the other two ligands. Therefore, it can be deduced that syringin still holds the top position among the other ligands in binding to the receptor in sites which are more energetically

favourable than cordifoline and palmatoside G respectively as having more number of hydrogen bonds means that the ligand has specifically a stronger affinity in binding to sites of the desired receptor chosen. Thus, syringin exhibits the highest potential to bind to the receptor 4L8Z and in turn inhibit it so that the family of Hsp90 protein gets downregulated and in turn the factors leading to cancer progressions cease resulting in tumor cell death.

### 3.2. Discussion:

The research conducted during the molecular docking of phytoconstituents from TC with receptors such as Bcl2, IAP-like proteins, Hsp90, and Ubiquitin ligase enzymes, which are known to be overexpressed during cancer progression, is unprecedented. To the best of our knowledge, no existing literature has reported a study of this nature up to this point in time. Though few literatures such as Herowati and Widodo, 2014 has provided evidences regarding the molecular docking of magnoflorin, cordiofolioside A, and syringin which revealed that they exhibited good binding interaction to catalytic site of glycogen phosphorylase. Sagar and Kumar, 2020 reported that Berberine, Isocolumbin, Magnoflorine, and Tinocordioside showed high binding efficacy against SARS-CoV-2 targets. *In-vitro* studies suggest that TC extracts have been found to show antitumor effects against glioblastoma, neuroblastoma, liver cancer, prostate cancer, cervical cancer, and a range of other cancers. Palmieri *et al.*, 2019 isolated Berberine from the stem of TC which was able to show time and dose-dependent downregulation of thirty-three out of total forty-four genes in the cell line of human colon adenocarcinoma (HCA-7), implicated in the cell cycle, differentiation, and epithelial mesenchymal transformation. Jagetia and Baliga, 2004; Wu *et al.*, 2012 suggested that Columbine, a furanolactone diterpenoid, showed chemopreventive potential against human colon cancer. Ludas *et al.*, 2019; Rashmi *et al.*, 2019 and Verma *et al.*, 2020 found that Chloroform and methanol fraction of TC stem (TCCF) exhibits an anti-cancerous effect through ROS generation against human breast cancer cells due to presence of phyto-constituents like quercetin and rutin. TCCF was shown to be an inducer of apoptosis by regulating pro and anti-apoptotic markers. Therefore, treatment of cells with TCCF and methanol extract showed reduced colony-forming capability and enhanced intracellular ROS production. The phyto-constituents identified of TC extract were alkaloids, diterpenoid lactones, steroids, glycosides, and aliphatics. TC and its phytochemicals are reported as very potent anticancer drugs. TC was proved to be effective in several other tumour models as well including Ehrlich ascites carcinoma (EAC) in mice. It induces proliferation and myeloid differentiation of bone marrow precursor cells in a tumour-bearing host and activates the tumour-associated macrophages-derived dendritic cells. Mitra *et al.*, 2019 found that TC in conjunction with gamma radiation may provide an effective remedial strategy for cancer because of its effectiveness against various cancers and inhibition of experimental metastasis. This present study suggests that syringin, neotigogenin and cordifolin in comparison to the other mentioned phytochemicals show maximum potential to inhibit the

receptors 2022, 1X0X, 4AUQ, and 4L8Z, thus downregulating their mechanism in progression of cancer.

#### 4. CONCLUSION

Molecular docking of several known phyto-constituents of TC with 3D structures of anti-apoptotic protein receptors that are commonly over-expressed during cancer progression like Bcl2, IAP, Ubiquitin ligases and HSP90 in Molegro Virtual Docker and their 3D as well as 2D visualization in Discovery studio has yielded the following conclusion that syringin, neotigenin and cordifolin has shown maximum number of interactions with the afore-mentioned receptors. Therefore, their practical applications on treatment of cancer both *in-vivo* and *in-vitro* might prove fruitful in future prospects.

**Acknowledgment:** We acknowledge the Department of Biotechnology (DBT), Government of India for using resources of ongoing DBT project (No. BT/INF/22/SP45376/2022) in the present work. Additionally, we would like to express our gratitude to Cotton University's Faculty of Life Sciences for providing the animal housing facility.

**Conflicts of interest:** The authors declare that they have no known competing financial interests or personal relationships that could have appeared to influence the work reported in this paper.

#### REFERENCES

1. Agrawal SN. 2019. The Vital Phenomena of Apoptosis: A Review. *South Asian Research Journal of Medical Sciences*. **1**(1): 15-19
2. Jan R and Chaudhry GS. 2019. Understanding Apoptosis and Apoptotic Pathways Targeted Cancer Therapeutics. *Advanced Pharmaceutical Bulletin*. **9**(2): 205-218.
3. Adams JM and Cory S. 1998. *Science*. **281**(1322–1326).
4. Kelekar A and Thompson CB. 1998. *Trends in Cellular Biology*. **8**(324–330).
5. Chao DT and Korsmeyer SJ. 1998. *Annual Review in Immunology*. **16**(395–419).
6. Reed JC. 1999. *Current Opinion in Oncology*. **11**(68–75).
7. Yang E, Zha J, Jockel J, Boise LH, Thompson CB, and Korsmeyer, SJ. 1995. *Cell*. **80**(285–291).
8. Thompson CB. 1995. *Science*. **267**(1456–1462).
9. Kusenda J. 1998. *Neoplasma* (Bratisl.). **45**(117–122).
10. Strasser A, Huang CS and Vaux DL. 1997. *Biochimica Et Biophysica Acta*. **1333**(151–178).
11. Berghella AM, Pellegrini P, Contasta I, Del Beato T. and Adorno D. 1998. *Cancer Biotherapy and Radiopharmaceuticals*. **13**(225–236).
12. Nicholson DW. 2000. *Nature* (London). **407**(810 – 816).
13. Piche A, Grim J, Rancourt C, Gomez-Navarro J, Reed JC and Curiel DT. 1998. *Cancer Research*. **58**(2134–2140).

14. Wang JL, Zhang ZJ, Choksi S, Shan S, Lu Z, Croce CM, Alnemri ES, Kornegold R and Huang Z. 2000. *Cancer Research*. **60**(1498–1502).
15. Wang JL, Liu D, Zhang ZJ, Shan S, Han X, Srinvasula SM, Croce CM, Alnemri ES, and Huang Z. 2000. *Proceedings of the National Academy of Sciences*. **97**(7124–7129).
16. Hershko A and Ciechanover A. 1998. The ubiquitin system. *Annual Review Biochemistry*. **67**(425-479).
17. Li W, Bengtson MH, Ulbrich A, Matsuda A, Reddy VA, Orth A, Chanda SK, Batalov S and Joazeiro CA. 2008. Genome-wide and functional annotation of human E3 ubiquitin ligases identifies MULAN, a mitochondrial E3 that regulates the organelle's dynamics and signaling. *PLoS One*. **3**(e1487).
18. Hanahan D and Weinberg RA. 2011. Hallmarks of cancer: the next generation. *Cell*. **144**(646-674),
19. Qi J, and Ronai ZA. 2015. Dysregulation of ubiquitin ligases in cancer. *Drug Resistance Updates*, **23**(1-11).
20. Duan S and Pagano M. 2021. Ubiquitin ligases in cancer: Functions and clinical potentials. *Cell Chemical Biology*. **28**(7):918-933
21. Shin H, Renatus M, Eckelman BP, Nunes VA, Claudio A, Sampaio M and Salvesen GS. 2005. The BIR domain of IAP-like protein 2 is conformationally unstable: implications for caspase inhibition. *Biochemical Journal*. **385**(1–10).
22. Uren AG, Coulson EJ, and Vaux DL. 1998. Conservation of baculovirus inhibitor of apoptosis repeat proteins (BIRPs) in viruses, nematodes, vertebrates, and yeasts. *Trends in Biochemical Sciences*. **23**(159–162).
23. Deveraux QL and Reed JC. 1999. IAP family proteins – suppressors of apoptosis. *Genes Development*. **13**(239–252).
24. Salvesen GS and Duckett CS. 2002. IAP proteins: blocking the road to death's door. *Nature Reviews Molecular Cell Biology*. **3**(401–410).
25. Deveraux Q, Takahashi R, Salvesen GS, and Reed JC. 1997. X-linked IAP is a direct inhibitor of cell death proteases. *Nature (London)*. **388**(300–304).
26. Roy N, Deveraux QL, Takahashi R, Salvesen GS and Reed JC. 1997. The c-IAP-1 and c-IAP-2 proteins are direct inhibitors of specific caspases. *EMBO Journal*. **16**(6914–6925).
27. Maier JK, Lahoua Z, Gendron NH, Fetni R, Johnston A, Davoodi J, Rasper D, Roy S, Slack RS, Nicholson DW and MacKenzie AE. 2002. The neuronal apoptosis inhibitory protein is a direct inhibitor of caspases 3 and 7. *Journal of Neuroscience*. **22**(2035–2043).
28. Vucic D, Stennicke HR, Pisabarro MT, Salvesen GS and Dixit VM. 2000. ML-IAP, a novel inhibitor of apoptosis that is preferentially expressed in human melanomas. *Current Biology*. **10**(1359–1366).
29. Kasof GM and Gomes BC. 2001. Livin, a novel inhibitor-of-apoptosis (IAP) family



- member. *Journal of Biological Chemistry*. **276**(3238–3246).
30. Conway EM, Pollefeyt S, Cornelissen J, DeBaere I, Steiner-Mosonyi M, Ong K, Baens M, Collen D and Schuh AC. 2000. Three differentially expressed survivin cDNA variants encode proteins with distinct antiapoptotic functions. *Blood*. **95**(1435–1442).
  31. Shin S, Sung BJ, Cho YS, Kim HJ, Ha NC, Hwang JI, Chung CW, Jung YK and Oh BH. 2001. An anti-apoptotic protein human survivin is a direct inhibitor of caspase-3. *Biochemistry*. **40**(1117–1123).
  32. Bartke T, Pohl C, Pyrowolakakis G and Jentsch S. 2004. Dual Role of BRUCE as an antiapoptotic IAP and a chimeric E2/E3 ubiquitin ligase. *Molecular Cell*. **14**(801–811).
  33. Richter BW, Mir SS, Eiben LJ, Lewis J, Reffey SB, Frattini A, Tian L, Frank S, Youle RJ and Nelson DL. 2001. Molecular cloning of ILP-2, a novel member of the inhibitor of apoptosis protein family. *Molecular and Cellular Biology*. **21**(4292–4301).
  34. Lagace M, Xuan JY, Young SS, McRoberts C, Maier J, Rajcan-Separovic E, and Korneluk RG. 2001. Genomic organization of the X-linked inhibitor of apoptosis and identification of a novel testis-specific transcript. *Genomics*. **77**(181–188).
  35. Verhagen AM, Coulson EJ and Vaux DL. 2001. Inhibitor of apoptosis proteins and their relatives: IAPs and other BIRPs. *Genome Biology*. **2**(7):3009.1-3009.10
  36. Takahashi R, Deveraux Q, Tamm I, Welsh K, Assa-Munt N, Salvesen GS and Reed JC. 1998. A single BIR domain of XIAP sufficient for inhibiting caspases. *Journal of Biological Chemistry*. **273**(7787–7790).
  37. Sun C, Cai M, Meadows RP, Xu N, Gunasekera AH, Herrmann J, Wu JC and Fesik SW. 2000. NMR structure and mutagenesis of the third BIR domain of the inhibitor of apoptosis protein XIAP. *Journal of Biological Chemistry*. **275**(33777–33781).
  38. Abdullah H, Marwan EEL-S and Hassan YN. 2018. The HSP90 Family: Structure, Regulation, Function, and Implications in Health and Disease. *International Journal of Molecular Sciences*. **19**(9):2560. doi: 10.3390/ijms19092560
  39. Whitesell L and Lindquist SL. 2005. HSP90 and the chaperoning of cancer. *Nature Reviews Cancer*. **5**(761–772). doi: 10.1038/nrc1716.
  40. Miyata Y, Nakamoto H, and Neckers L. 2013. The therapeutic target Hsp90 and cancer hallmarks. *Current Pharmaceutical Design*. **19**(347–365). doi: 10.2174/138161213804143725
  41. Vartholomaïou E, Echeverría PC and Picard D. 2016. Unusual Suspects in the Twilight Zone Between the Hsp90 Interactome and Carcinogenesis. Hsp90 in Cancer: Beyond the Usual Suspects. *Advances in Cancer Research*. **129**(1–30).
  42. Chen B, Zhong D and Monteiro A. 2006. Comparative genomics and evolution of the HSP90 family of genes across all kingdoms of organisms. *BMC Genomics*. **7**:156. doi: 10.1186/1471-2164-7-156.
  43. Lewis M, Bagwill C, Hardebeck L and Wireduuah S. 2016. Modern Computational Approaches to Understanding Interactions of Aromatics. *Aromatic Interactions: Frontiers in Knowledge and Application*. England: Royal Society of Chemistry. 1–17
  44. Martinez CR and Iverson BL. 2012. Rethinking the term pi-stacking. *Chemical Science*. **3**(7). doi:10.1039/c2sc20045g
  45. Huber RG, Margreiter MA, Fuchs JE, von Grafenstein S, Tautermann CS, Liedl KR and Fox T 2014. Heteroaromatic  $\pi$ -stacking energy landscapes. *Journal of Chemical Information and Modeling*. **54** (5): 1371–1379
  46. Dougherty DA and JC Ma. 1997. The Cation– $\pi$  Interaction. *Chemical Reviews*. **97** (5): 1303–1324.
  47. Herowati R and Widodo GP. 2014. Molecular Docking Studies of Chemical Constituents of *Tinospora cordifolia* on Glycogen Phosphorylase. *Procedia Chemistry* **13**:63-68.
  48. Sagar V and HS Kumar A. (2020). Efficacy of Natural Compounds from *Tinospora cordifolia* against SARS-CoV-2 Protease, Surface Glycoprotein and RNA Polymerase. *Biology, Engineering, Medicine and Science Reports*, **6**(1):06–08.
  49. Palmieri A, Scapoli L, Iapichino A, et al (2019) Berberine and *Tinospora cordifolia* exert a potential anticancer effect on colon cancer cells by acting on specific pathways. *International Journal of Immunopathological Pharmacology*. **33**. <https://doi.org/10.1177/2058738419855567>
  50. Jagetia GC, Baliga MS (2004) The evaluation of nitric oxide scavenging activity of certain Indian medicinal plants in vitro: A preliminary study. *Journal of Medicinal Food*. <https://doi.org/10.1089/jmf.2004.7.34> 3–52.
  51. Wu K, Yang Q, Mu Y, et al. (2012). Berberine inhibits the proliferation of colon cancer cells by inactivating Wnt/ $\beta$ -catenin signaling. *International Journal of Oncology*. **292**-298. <https://doi.org/10.3892/ijo.2012.1423>
  52. Ludas A, Indu S, Hinduja S, et al (2019) Anti-cancer potential of polysaccharide isolated from methanolic extract of *Tinospora cordifolia* stem bark. *International Journal of Pharmaceutical Sciences*. **11**(5):43-47
  53. Rashmi KC, Harsha Raj M, Paul M, et al (2019) A new pyrrole-based small molecule from *Tinospora cordifolia* induces apoptosis in MDA-MB-231 breast cancer cells via ROS mediated mitochondrial

- damage and restoration of p53 activity. *Chemico-Biological Interactions*. **299**(120-130)
54. Verma DK, Goyal K, Kumar P, El-Shazly M (2020) Unmasking the Many Faces of Giloy (*Tinospora cordifolia* L.): A fresh look on its phytochemical and medicinal properties. *Current Pharmaceutical Design*. **27**(22):2571-2581
55. Mitra S, Nguyen LN, Akter M, et al (2019) Impact of ROS generated by chemical, physical, and plasma techniques on cancer attenuation. *Cancers*. **11**(7):1030.